J. Fluid Mech. (1972), *vol.* 51, *part* 3, *pp.* 417–433
Printed in Great Britain

Numerical solution of the Navier–Stokes equations for symmetric laminar incompressible flow past a parabola

By R. T. DAVIS

Department of Aerospace Engineering and Applied Mechanics,
University of Cincinnati

(Received 17 February 1971 and in revised form 18 May 1971)

Symmetric laminar incompressible flow past a parabolic cylinder is considered for all Reynolds numbers. In the limit as the Reynolds number based on nose radius of curvature goes to zero, the solution for flow past a semi-infinite flat plate is obtained. All solutions are found by using an implicit alternating direction method to solve the time-dependent Navier–Stokes equations. The solutions found are compared with various other exact and approximate solutions. Results are presented for skin friction, surface pressure, friction drag and pressure drag. The numerical method developed is of particular interest since it combines the alternating direction method with the implicit method for solving the boundary-layer equations. This leads to fast convergence and may be of use in other problems.

1. Introduction

Exact numerical solutions to the Navier–Stokes equations are now possible using various numerical techniques, and yet some of the simplest flow problems of great importance such as flow past parabolas, wedges, flat plates, paraboloids and cones have received little attention. In this paper we present solutions for flow past parabolic cylinders and, in the limit of zero Reynolds number, flow past the semi-infinite flat plate. Dennis & Walsh (1971) and Botta, Dijkstra & Veldman (1971) also considered the parabola problem while van de Vooren & Dijkstra (1970) and Yoshizawa (1970) have considered the zero Reynolds number case of flow past a semi-infinite flat plate. The present study presents additional details of the flow field along with comparisons with other work by Van Dyke (1964, 1972) and Davis (1967). The numerical method presented may be useful in solving other problems involving the Navier–Stokes equations since it combines the numerical technique developed by Blottner & Flügge-Lotz (1963) for solving the boundary-layer equations with the implicit alternating direction method developed by Douglas (1955).

Careful attention is focused on extracting singularities from the problem in the limit as Reynolds number goes to zero, and a set of dependent and independent variables are presented which seem ideally suited to the present problem.

A technique similar to the one presented here is being used by the author to solve the problem of laminar incompressible flow past a paraboloid. Similar techniques may be possible in the wedge and cone problems. These problems are

of importance in properly determining the local solutions near leading edges in more complicated problems. The singularities which exist in such flows are usually ignored by those who study numerical solutions to the Navier–Stokes equations.

2. Governing equations and boundary conditions

In a previous paper (Davis 1967) the advantages of using parabolic co-ordinates in the problem of laminar flow past a semi-infinite flat plate were discussed. It is equally advantageous to use the same co-ordinate system for flow past a parabola, and the flat plate solution is contained as the limiting solution as the Reynolds number based on the nose radius of curvature goes to zero. Since the steady-state numerical solution will be determined as the limiting solution to the unsteady equations for large time, the governing equations are given including the unsteady terms.

In non-dimensional parabolic co-ordinates the unsteady Navier–Stokes equations are expressed in terms of the stream function and vorticity as

$$\left[\frac{\partial^2}{\partial\xi^2}+\frac{\partial^2}{\partial\eta^2}+\psi_\xi\frac{\partial}{\partial\eta}-\psi_\eta\frac{\partial}{\partial\xi}-(\xi^2+\eta^2)\frac{\partial}{\partial t}\right]\omega=0 \tag{2.1}$$

and

$$\frac{\partial^2\psi}{\partial\xi^2}+\frac{\partial^2\psi}{\partial\eta^2}=-(\xi^2+\eta^2)\,\omega, \tag{2.2}$$

where the stream function ψ is non-dimensionalized by the kinematic viscosity ν and the vorticity ω is non-dimensionalized by the free-stream velocity squared divided by the kinematic viscosity, i.e. U^2/ν. The independent variables ξ and η (parabolic co-ordinates) are non-dimensionalized and related to the dimensional x and y Cartesian co-ordinates by

$$x+iy=\nu(\xi+i\eta)^2/2U \tag{2.3a}$$

or

$$x=\nu(\xi^2-\eta^2)/2U,\quad y=\nu\xi\eta/U. \tag{2.3b,c}$$

Finally, the time t is non-dimensionalized by ν/U^2.

The boundary conditions on the problem can be written as

$$\psi(\xi,R^{\frac{1}{2}})=0,\quad \partial\psi(\xi,R^{\frac{1}{2}})/\partial\eta=0, \tag{2.4a,b}$$

and

$$\psi(\xi,\eta)\sim\xi\eta\quad\text{as}\quad\eta\to\infty, \tag{2.5}$$

where

$$R=Ua/\nu, \tag{2.6}$$

a being the nose radius of curvature of the parabola. Note that the body surface is located at $\eta=R^{\frac{1}{2}}$.

The following variables are introduced to remove singularities in the numerical solution. The Stokes solution with minimum singularity at the leading edge suggests that the vorticity is singular at the leading edge of the flat plate.† We

† The Stokes solution near the nose of a parabola shows that $\psi=A\xi(\eta-R^{\frac{1}{2}})^2$, where A is an undetermined constant. From this expression the vorticity ω is found to be

$$-2A\xi/(\xi^2+\eta^2)$$

and the pressure P, non-dimensionalized by ρU^2, is found to be $2A\eta/(\xi^2+\eta^2)+C$.

also know that the vorticity is an odd function of the co-ordinate ξ. In addition we find that far downstream the following form reduces to the proper form for vorticity for the Blasius boundary-layer equation. Thus we let

$$\omega = -[\xi/(\xi^2+\eta^2)]\,g(\xi,\eta). \tag{2.7}$$

In a like manner we introduce a new form for the stream function. Making use of the condition on the stream function at infinity (2.5), the Stokes and Oseen solutions, the fact that the stream function must be an odd function of ξ and examining the proper form for the stream function far downstream we write

$$\psi = \xi f(\xi,\eta). \tag{2.8}$$

With the new dependent variables given by (2.7) and (2.8) the governing equations (2.1) and (2.2) become

$$g_{\eta\eta}+\left(f+\xi f_\xi-\frac{4\eta}{\xi^2+\eta^2}\right)g_\eta+\frac{1}{\xi^2+\eta^2}[(\xi^2-\eta^2)f_\eta-2\eta(f+\xi f_\xi)]\,g$$
$$-\left(\xi f_\eta+\frac{4\xi}{\xi^2+\eta^2}\right)g_\xi-(\xi^2+\eta^2)\,g_t+g_{\xi\xi}+\frac{2}{\xi}g_\xi=0 \tag{2.9}$$

and

$$f_{\eta\eta}-g+f_{\xi\xi}+(2/\xi)f_\xi=0, \tag{2.10}$$

with boundary conditions

$$f(\xi,R^{\frac{1}{2}})=0,\quad f_\eta(\xi,R^{\frac{1}{2}})=0, \tag{2.11a,b}$$

$$f(\xi,\eta)\sim\eta,\quad g(\xi,\eta)\sim 0,\quad \text{as}\quad \eta\to\infty. \tag{2.12a,b}$$

In addition symmetry conditions must be applied on f and g at $\xi=0$.

It should be noted that these equations reduce to the form used by Davis (1967) for obtaining locally similar solutions when the terms with ξ and t derivatives are neglected. It should also be noted that the equations are parabolic in ξ when the last two terms in both (2.9) and (2.10) are neglected. This fact will be exploited in the numerical solution. In fact neglecting these terms results in equations which contain both the first-order boundary-layer terms and the terms for the second-order curvature corrections. The numerical scheme to be used will take advantage of this and results in a solution technique which will converge rapidly, especially at high Reynolds numbers.

In order to evaluate the pressure on the parabola or flat plate surface, it is necessary to find an expression for the pressure in terms of vorticity. This is done by writing the ξ momentum equation in parabolic co-ordinates and evaluating the resulting equation on the body surface. This results in

$$\frac{\partial P}{\partial\xi}=\frac{\xi}{\xi^2+\eta^2}\left[\frac{\partial g}{\partial\eta}-\frac{2\eta}{\xi^2+\eta^2}g\right]\quad\text{at}\quad\eta=R^{\frac{1}{2}}, \tag{2.13}$$

where P is defined to be the dimensional pressure minus the free-stream pressure non-dimensionalized by ρU^2. The value of P as $\xi\to\infty$ can be shown to be zero. Thus using the pressure at downstream infinity as a boundary condition, the surface pressure can be found by integrating from downstream infinity back along the surface. There are certain difficulties in evaluating the pressure and the drag integrals which follow. These difficulties will be discussed in § 5.

The friction and pressure drags are given by

$$D_f = 2\int_0^s \tau_w \cos\theta \, ds \tag{2.14}$$

and

$$D_P = 2\int_0^s P_w \sin\theta \, ds, \tag{2.15}$$

where θ is the parabola surface slope, s is the arc length along the parabola, and τ_w and P_w are the dimensional surface shear and pressure respectively.

Non-dimensionalizing (2.14) and (2.15) and substituting the relations for the parabolic co-ordinate transformations, we obtain

$$C_{Df} = \frac{D_f}{\mu U} = 2\int_0^{\xi} \frac{\xi^2}{\xi^2 + R} g(\xi, R^{\frac{1}{2}}) d\xi \tag{2.16}$$

and

$$C_{DP} = \frac{D_P}{\mu U} = 2R^{\frac{1}{2}} \int_0^{\xi} P(\xi, R^{\frac{1}{2}}) d\xi. \tag{2.17}$$

Finally an expression for the skin friction coefficient can be written as

$$C_f = \frac{\tau_w}{\rho U^2} = \frac{\xi}{\xi^2 + R} g(\xi, R^{\frac{1}{2}}). \tag{2.18}$$

3. Previous approaches to the flat plate and parabola problem

We will not discuss in detail the various asymptotic results which were discussed previously by Davis (1967) for the flat plate problem but will point out new results which have been discovered since then.

Van de Vooren & Dijkstra (1970) presented a numerical solution to the flat plate problem. They were quite careful in handling the boundary conditions at infinity for both the ξ and η directions. They did this by introducing independent variables which transformed the problem in the quarter infinite region to one in a finite region. We believe their solution to be quite accurate and to model correctly the flat plate problem. Later we will show that our flat plate results are in close agreement with those of van de Vooren & Dijkstra.

Yoshizawa (1970) also solved the flat plate problem in a manner somewhat similar to that used by van de Vooren & Dijkstra (1970). Some questions might arise as to the inaccuracy in imposing the free-stream and downstream conditions at rather small values of ξ and η. Since the stream function approaches its free-stream and downstream conditions with terms which die out algebraically (the higher-order boundary-layer results of Imai (1957), for example, indicate this), one should go to a quite large value of ξ and η (infinite preferably) before imposing the outer boundary conditions. Approaches which do not do this lead to errors in the solution which are difficult to assess. Apart from this, Yoshizawa's solution appears to be quite satisfactory and agrees closely with the results of van de Vooren & Dijkstra (1970) for leading edge skin friction.

Dennis & Walsh (1971) have computed flows past parabolas at various Reynolds numbers. The method they used is similar to one discussed by Dennis & Chang (1969). Van Dyke (1972) has used the solutions of van de Vooren &

Dijkstra (1970) and Yoshizawa (1970) for the flat plate to obtain the low Reynolds number solution for flow past a parabola. He then used his second-order boundary layer solution (Van Dyke 1964) to combine with the low Reynolds number solution to form a rational fraction for leading edge skin friction which agrees well with the results of Dennis & Walsh (1971) for all Reynolds numbers. Botta *et al.* (1971) have also made calculations for the parabola which agree with Dennis & Walsh (1971) and Van Dyke (1972).

Although van de Vooren & Dijkstra (1970) have shown, using their numerical results, that there is about a 5 % error near the leading edge in skin friction in the results of Davis (1967) and Dean (1954) it is felt that the results of Dean and Davis are quite acceptable, especially since there has been considerable controversy over whether the skin friction is zero, finite, or singular at the leading edge of a flat plate.

In this paper we will attempt to determine where the 5 % error occurs in the method of Davis (1967). Dijkstra (1969) has pointed out that Dean's (1954) method does not produce exponential decay of vorticity for large η. On the other hand it can be shown that in Davis's (1967) solution vorticity dies out exponentially, but the stream function can also be shown to die out exponentially to its free-stream condition. It is known that the stream function should die out algebraically. The fact that the stream function dies out exponentially in Davis's results can be seen from equation (2.10). The last two terms drop out in the first truncation. Thus if g dies out exponentially, so does $f_{\eta\eta}$. Applying the boundary condition at infinity (2.12a) shows that f does not have the proper behaviour. Higher truncations do not remedy the situation. Thus to handle the flow field properly far from the body the complete stream function equation should be used.

Finally, it should be pointed out that the presentation of the results of Davis (1967) in figure 1 of the paper by van de Vooren & Dijkstra (1970) is in error. The values plotted in the range above a Reynolds number of five are too high. This is obvious since in figure 2 van de Vooren & Dijkstra show an integrated skin friction by Davis which is below their value. This is impossible if their local skin friction is always lower than the values given by Davis as shown in figure 1. A correct plot would show values of local skin friction by Davis which drop slightly below van de Vooren & Dijkstra's values above Reynolds numbers of about five. This error probably occurs because of difficulty in picking skin friction values off the curves given by Davis (1967).

4. Numerical method of solution

The numerical method of solution of (2.9) and (2.10) will be similar to the alternating direction implicit method developed by Douglas (1955) for solving linear parabolic equations in two space variables. In solving non-linear parabolic equations, there is some choice in how the convective terms are to be handled and it is felt that the procedure to be employed here is novel in that respect. The method to be described may be useful in solving other problems involving the Navier–Stokes equations.

Equations (2.9) and (2.10) have been deliberately written in a form such that

locally similar solutions can be obtained directly by ignoring the ξ derivatives. We also note that if we exclude the last two terms in (2.9) and (2.10), i.e the terms $f_{\xi\xi}+2f_\xi/\xi$ and $g_{\xi\xi}+2g_\xi/\xi$, we obtain equations which include the second-order boundary-layer equations for flow over a parabola, which are formally valid to second order in the inverse square root of the Reynolds number for large Reynolds numbers. Making this approximation, we ignore the second-order effect of flow due to displacement thickness which can be incorporated by leaving in the last two terms in (2.10), i.e. $f_{\xi\xi}+2f_\xi/\xi$. We thus develop our difference scheme so that we are integrating boundary-layer-like equations at one half time step and correcting for displacement effects ($f_{\xi\xi}+2f_\xi/\xi$) and the elliptic terms in the vorticity equation ($g_{\xi\xi}+2g_\xi/\xi$) at the next half time step. This is done by writing (2.9) and (2.10) as follows. Note that a fictitious time derivative has been added to the stream function equation in order to employ the alternating direction method. We have also deleted the $(\xi^2+\eta^2)$ coefficient from the g_t term in (2.9) since this seemed to lead to faster convergence. If we were interested in unsteady solutions and not just the steady-state solution, this term would have to be retained. In the first half time step the equations are written as

$$\begin{aligned}(g^*-g_j)/\tfrac{1}{2}\Delta t = {} & g^*_{\eta\eta}+[f^*+\xi f^*_\xi-4\eta/(\xi^2+\eta^2)]g^*_\eta \\ & +[(\xi^2-\eta^2)f^*_\eta-2\eta(f^*+\xi f^*_\xi)]g^*/(\xi^2+\eta^2) \\ & -[\xi f^*_\eta+4\xi/(\xi^2+\eta^2)]g^*_\xi+[g_{\xi\xi}+2g_\xi/\xi]_j \qquad (4.1)\end{aligned}$$

and

$$(f^*-f_j)/\tfrac{1}{2}\Delta v = f^*_{\eta\eta}-g^*+[f_{\xi\xi}+2f_\xi/\xi]_j, \qquad (4.2)$$

where Δv is a fictitious time step increment. The starred (*) variables are evaluated at the unknown new half time step and the quantities with subscripts j are evaluated at the previous half time step. At the next half time step the time derivatives are written as $(g_{j+1}-g^*)/\frac{1}{2}\Delta t$ and $(f_{j+1}-f^*)/\frac{1}{2}\Delta v$ and now the starred variables become known quantities and the quantities on the right-hand side of (4.1) and (4.2) with subscripts j become $j+1$ and thus become the unknowns.

The equations have been written in this particular form since the starred variables contain the boundary-layer equations. At the time step where the starred variables are the unknowns, the equations in the spatial co-ordinates are integrated as boundary-layer equations using an implicit finite-difference method similar to the one developed by Blottner & Flügge-Lotz (1963). All η derivatives in the starred variables are written as three-point central differences and the ξ derivatives in the starred variables are written as two-point backward differences. The spatial solution in starred variables is started at the stagnation point or leading edge of the parabola where the equations in starred variables reduce to ordinary differential equations in η. The stagnation-point or leading-edge solution is then found through iteration by first putting in guessed values for the non-linear coefficients and then iterating until the solution converges. A good initial guess on the coefficients is the solution from the previous time step. This procedure is repeated at each downstream station along the parabola surface. The method described for this half time step is a rather standard procedure for solving the boundary-layer equation and has been employed by numerous authors.

At the next half time step the starred variables become known quantities and the unstarred ones unknown. The ξ derivatives in the last two terms of (4.1) and (4.2) are replaced by three-point central differences, and the solution is obtained as before except now we are dealing with a linear problem and no iteration is required.

Some mention should be made of special problems which arise in the solution. In both half time steps simultaneous equations of triadiagonal form are encountered which are easily solved by using the Thomas (1949) algorithm. In order to use this method, the boundary conditions must be put in a suitable form.

For solving in the starred variables the vorticity equation (4.1) is uncoupled from the stream function equation (4.2) if the values from the previous iteration at a particular station are used for the f^* terms appearing in the coefficients. The vorticity equation (4.1) in starred variables can then be solved at a particular station if a value of $g^*(\xi, R^{\frac{1}{2}})$ is guessed. This is necessary since only $g^*(\xi, \infty)$ is given as a boundary condition (see (2.11) and (2.12)). Next the stream function equation (4.2) is solved in starred variables. Note that boundary conditions on f^* are given at both $\eta = R^{\frac{1}{2}}$ and $\eta = \infty$ by (2.11*a*) and (2.12*a*); however, in addition, the condition (2.11*b*) must be satisfied on the body surface. This is done by repeating the solution, guessing a new value for $g^*(\xi, R^{\frac{1}{2}})$ and superimposing the previous solution so that condition (2.11*b*) is satisfied. This determines the correct value of vorticity on the surface.

At the next half time step, initial conditions are needed at $\xi = 0$ for the vorticity and stream function equations. These are obtained by evaluating both (4.1) and (4.2) at $\xi = 0$. To do this, we need the limiting values of f_ξ/ξ and g_ξ/ξ as $\xi \to 0$; these are given by $f_{\xi\xi}$ and $g_{\xi\xi}$. Combining these terms with the $f_{\xi\xi}$ and $g_{\xi\xi}$ terms already appearing, writing these terms as three-point central differences, and making use of the symmetry of the f and g functions with respect to $\xi = 0$, we obtain a boundary condition at $\xi = 0$ for both the vorticity and stream function equations. The solution for flow past a parabola is known to approach the flat plate Blasius solution as $\xi \to \infty$. This boundary condition is applied at downstream infinity.

The outer boundary conditions present a problem since they must be prescribed at infinity. In the numerical solutions, vorticity is found to die out exponentially with η as it should; however, the stream function is found to die out algebraically. Thus, to ensure numerical accuracy, we impose the boundary condition on stream function at infinity whereas it is not so important to impose the vorticity condition at infinity. To do this we must transform the infinite η region to a finite region. Van de Vooren & Dijkstra (1970) investigated the proper form for the transformation and proposed a new normal co-ordinate variable. We have also looked at this problem and find that if we let

$$\eta = [5N/(1-N)] + R^{\frac{1}{2}}, \tag{4.3}$$

we can get an accurate solution with fewer points than was possible from the transformation used by van de Vooren & Dijkstra (1970). In our new variables N goes from zero to one whereas η goes from zero to infinity. The value 5 appears in the numerator since this gives a value of $\eta = 5 + R^{\frac{1}{2}}$ when $N = 0{\cdot}5$. The vorticity is found to go to zero at about $N = 0{\cdot}5$ for all Reynolds numbers and thus half

the grid covers the viscous region and the other half the region which is outside this viscous region. The expression (4.3) can be shown to handle singularities as $\eta \to \infty$ properly, see van de Vooren & Dijkstra (1970).

Van de Vooren & Dijkstra (1970) have also examined transformations in the ξ variable which will have the proper behaviour as $\xi \to \infty$ and transform the infinite ξ region into a finite region. These transformations have the form

$$s = 1 - \left[\log\left(1 + \frac{\xi}{A}\right) \Big/ \frac{\xi}{A}\right], \tag{4.4}$$

where van de Vooren & Dijkstra chose A to be 2 for the flat plate case. Note that s (which is not the arc length along the parabola) runs from 0 at $\xi = 0$ to 1 at $\xi = \infty$. From the numerical solutions we have determined A such that s equals 0·5 when the skin friction function $g(\xi, R^{\frac{1}{2}})$ is approximately half way between its value at the stagnation point and $\xi = \infty$. A relation which does this approximately is

$$A = 4 + 0{\cdot}4\, R^{\frac{1}{2}}. \tag{4.5}$$

With the transformation of the independent variables given by (4.3) and (4.4), the governing equations (2.9) and (2.10) are now confined to a finite region extending from s and $N = 0$ to 1. The calculations were performed with different combinations of step sizes; however, the final results are for 125 steps in the N direction and 40 steps in the s direction. Little difference was found between these results and those obtained using 20 steps in the s direction. Tests of step sizes in the normal direction showed that 125 steps were sufficient for three-place accuracy.

We note from (2.12a) that the function $f \to \infty$ like η as $\eta \to \infty$. This was handled in the numerical calculations by defining a new function h,

$$h = f - \eta. \tag{4.6}$$

We know that the displacement effects are such that h goes to infinity like a constant term plus terms which die out algebraically. To treat this properly we prescribe the boundary condition

$$h_\eta(\xi, \infty) = 0. \tag{4.7}$$

If we wanted a true unsteady solution, it would be necessary to relax the stream function equation (4.2) at each time step Δt by marching in Δv until a steady-state solution with respect to v were obtained; however, since we are only interested in the final steady-state solution to the problem, the solutions to the two equations were found by marching simultaneously with steps in Δt and Δv. Experimentally, approximate optimal time steps of Δt and Δv of ten were found for the case of Reynolds number of ten and the same Δt and Δv step sizes were used for all other cases. The rate of convergence depended on Reynolds number with faster convergence being obtained at high Reynolds numbers, as should be obvious from the way the numerical solution is formulated. Solutions started at t and $v = 0$ were obtained by ignoring the time and last two ξ spatial terms in the transformed form of (2.9) and (2.10). This set of parabolic partial differential equations was then integrated from $\xi = 0$ to ∞ in exactly the same manner as in the star step of the alternating direction method described previously. The

solution of this set of equations at infinity, which is the flat plate solution, was then used as a downstream boundary condition and the other solution points were used as an initial solution. This is an accurate initial solution and is exact in the limit as Reynolds number goes to infinity. The numbers obtained from the starting solution are quite close to the locally similar solution obtained by Davis (1967), the difference being that the parabolic ξ derivative term in (2.9) is neglected in the locally similar solutions.

Convergence to three-place accuracy is obtained typically in ten to twenty time steps resulting in a computing time on the IBM 360-50-65 computer of about ten minutes per value of Reynolds number in the case where 125 steps are taken in the normal N direction and 20 steps are taken in tangential s direction. Computing time was approximately twice as long for the cases where 40 steps were taken in the s direction. All calculations were done in double precision arithmetic.

5. Calculation of surface pressure and drag coefficients

As mentioned in § 2, the Stokes solution indicates that the pressure is singular at the leading edge of a flat plate. The expression for the pressure near the nose of a parabola from the Stokes solution is

$$P = [2A\eta/(\xi^2+\eta^2)]+C, \tag{5.1}$$

where A and C are undetermined constants. It was also mentioned in § 2 that the Stokes solution for vorticity gives

$$\omega = -2A\xi/(\xi^2+\eta^2). \tag{5.2}$$

Comparing (5.2) with (2.7), we see that at low Reynolds numbers

$$2A = g(0, R^{\frac{1}{2}}). \tag{5.3}$$

Thus to remove the singularity from the pressure expression we let

$$P = \frac{g(0, R^{\frac{1}{2}})\eta}{\xi^2+\eta^2} + \bar{P}(\xi, \eta). \tag{5.4}$$

Substituting into expression (2.13) we obtain

$$\frac{\partial \bar{P}}{\partial \xi} = \frac{\xi}{\xi^2+\eta^2}\left[\frac{\partial g}{\partial \eta} - \frac{2\eta}{\xi^2+\eta^2}(g-g_0)\right] \quad \text{at} \quad \eta = R^{\frac{1}{2}}, \tag{5.5}$$

where

$$g_0 = g(0, R^{\frac{1}{2}}). \tag{5.6}$$

The function $\bar{P}$ is properly behaved near $\xi = 0$. Numerical solutions obtained before this singularity was removed showed a large variation in pressure gradient $\partial P/\partial \xi$ near the stagnation point at low Reynolds numbers. It should also be noted that this transformation (5.4) encounters no difficulties as ξ goes to infinity or as Reynolds number goes to infinity.

We can now write down an expression for the pressure drag coefficient (2.17). With the new variables, this becomes

$$C_{DP} = 2R^{\frac{1}{2}}\left[g(0, R^{\frac{1}{2}})\tan^{-1}(\xi R^{-\frac{1}{2}}) + \int_0^{\xi} \bar{P}(\xi, R^{\frac{1}{2}})\, d\xi\right]. \tag{5.7}$$

For convenience, so that we will have a pressure drag coefficient which is finite at zero and infinite Reynolds numbers, we subtract the pressure drag contribution at infinite Reynolds number from (5.7) and divide the resulting expression by $R^{\frac{1}{2}}$.

The surface pressure distribution on the parabola as Reynolds number goes to infinity is given from inviscid theory as follows:

$$P_i = \tfrac{1}{2}R/(R+\xi^2). \tag{5.8}$$

The Reynolds number appears because the way we have non-dimensionalized is not appropriate for high Reynolds numbers. Thus subtracting out the drag at infinite Reynolds number and dividing by $R^{\frac{1}{2}}$ to obtain a finite limit as Reynolds number goes to zero or infinity, we obtain

$$\bar{C}_{DP} = 2\left[g(0,R^{\frac{1}{2}})\tan^{-1}(\xi R^{-\frac{1}{2}}) + \int_0^{\xi}[\bar{P}(\xi,R^{\frac{1}{2}}) - P_i(\xi,R^{\frac{1}{2}})]\,d\xi\right], \tag{5.9}$$

which results in

$$\bar{C}_{DP} = C_{DP}R^{-\frac{1}{2}} - R^{\frac{1}{2}}\tan^{-1}(\xi R^{-\frac{1}{2}}). \tag{5.10}$$

As ξ goes to infinity, (2.16) will result in a value of infinity for C_{Df} for finite values of Reynolds number. We avoid this by removing the infinite part of the integral. This is done by defining

$$\bar{C}_{Df} = 2\int_0^{\xi}\frac{\xi^2}{\xi^2+R}[g(\xi,R^{\frac{1}{2}}) - g(\infty,R^{\frac{1}{2}})]\,d\xi, \tag{5.11}$$

where $g(\infty,R^{\frac{1}{2}})$ can be shown to have the flat plate value of 0·4696. Comparing (5.11) with (2.17), we see that

$$\bar{C}_{Df} = C_{Df} - 2g(\infty,R^{\frac{1}{2}})[\xi - R^{\frac{1}{2}}\tan^{-1}(\xi R^{-\frac{1}{2}})]. \tag{5.12}$$

One can show from the results of Imai (1957) that $\bar{C}_{Df}$ should approach a value of 2·326 as ξ goes to infinity for the flat plate case. It would be more appropriate in (5.11) to subtract out the contribution to drag on the parabola at infinite Reynolds number. However since that solution can only be obtained numerically it will not be done. As a result C_{Df} will go to infinity like $R^{\frac{1}{2}}$ as Reynolds number goes to infinity.

With these expressions, the required integrations can be performed. In all cases, the trapezoidal rule is used; Simpson's rule was also used and showed insignificant difference in the results. Equation (5.5) is integrated by starting at $\xi = \infty$ and integrating back along the parabola surface to the leading edge. The remaining two integrals (5.9) and (5.11) are obtained by integrating from the leading edge to downstream infinity.

6. Results and conclusions

Figures 1 and 2 and table 1 give results for leading edge skin friction and pressure (see (2.18) and (5.4)) using the numerical method described in §4. Step sizes and convergence criteria were checked for a number of cases and it is felt that the quantities $g(0,R^{\frac{1}{2}})$ and $\bar{P}(0,R^{\frac{1}{2}})$ are probably accurate to three places. The same cannot be said for the friction and pressure drag coefficients $\bar{C}_{Df}(\infty,R^{\frac{1}{2}})$ and $\bar{C}_{DP}(\infty,R^{\frac{1}{2}})$ given in table 1 and figures 5 and 6. We found that these quanti-

ties were much more sensitive to step sizes and convergence criteria. This is because of the way they are defined. The expression (5.9) for $\bar{C}_{DP}$ is defined with the drag due to inviscid surface pressure subtracted out. Thus, $\bar{C}_{DP}$ is calculated, especially at high Reynolds numbers, from numbers which are in the fourth, fifth or even sixth significant figure of $\bar{P}(\xi, R^{\frac{1}{2}})$. The same is generally true of $\bar{C}_{Df}$ although not to the same extent as $\bar{C}_{DP}$, since only the flat plate value of g is subtracted out in (5.11). Thus, except for the flat plate case, the results of $\bar{C}_{Df}$ contain part of the first-order boundary-layer solution, which makes this result converge faster, even though it is not as useful as the result for $\bar{C}_{DP}$.

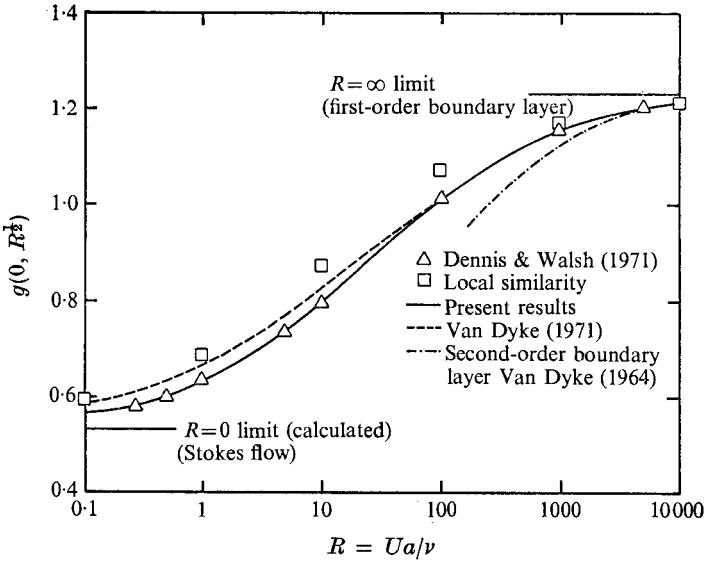

FIGURE 1. Skin friction at the leading edge of a parabolic cylinder.

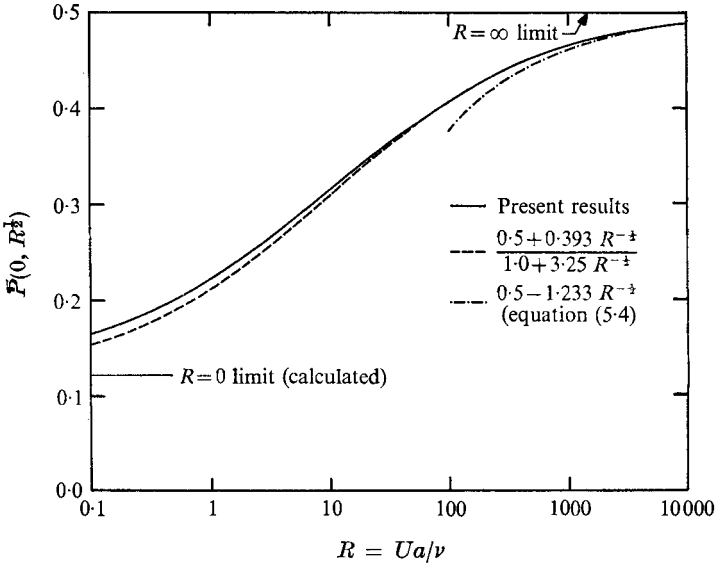

FIGURE 2. Pressure at the leading edge of a parabolic cylinder.

From the numerical results, we can find several limiting solutions. First, from (5.2) we find that the value of $2A$, which equals $g(0, R^{\frac{1}{2}})$ at low Reynolds numbers, can be evaluated from the flat plate solution to give

$$\omega = -0{\cdot}533\xi/(\xi^2+\eta^2) \tag{6.1}$$

near the leading edge of a parabola at low Reynolds number. From (5.4) and the numerical results, we can find an expression for pressure at low Reynolds number near the leading edge. This results in

$$P = [0{\cdot}533\eta/(\xi^2+\eta^2)] + 0{\cdot}121. \tag{6.2}$$

The numbers found from the numerical solutions to form these expressions are in excellent agreement with van de Vooren & Dijkstra (1970) and only slightly different from the results of Yoshizawa (1970) in the cases where they can be compared.

R	$g(0, R^{\frac{1}{2}})$	$\bar{P}(0, R^{\frac{1}{2}})$	$\dfrac{\bar{C}_{Df}(\infty, R^{\frac{1}{2}})}{1+R^{\frac{1}{2}}}$	$\bar{C}_{DP}(\infty, R^{\frac{1}{2}})$
0	0·533	0·121	2·411	2·770
0·1	0·563	0·165	2·475	2·805
0·3	0·586	0·187	2·499	2·829
1	0·629	0·221	2·516	2·846
3	0·694	0·262	2·523	2·882
10	0·793	0·313	2·507	2·931
30	0·899	0·362	2·483	2·938
100	1·009	0·408	2·451	2·902
300	1·089	0·441	2·427	2·839
1000	1·150	0·465	2·409	2·735
3000	1·186	0·479	2·401	2·661
10000	1·209	0·488	2·399	2·635

TABLE 1. Leading edge and drag integral results

From the expressions (5.7) and (5.9) and the numerical results, a low Reynolds number pressure drag coefficient can be found. The first term in (5.7) acts as a concentrated force at the leading edge even though its magnitude is only $R^{\frac{1}{2}}$. This can easily be evaluated and results in a value of $\pi g(0, R^{\frac{1}{2}})R^{\frac{1}{2}} = 1{\cdot}674R^{\frac{1}{2}}$. The remainder of the pressure drag comes from the drag on the body from the leading edge to downstream infinity. This is the second term in (5.7) and results in a calculated value of $1{\cdot}096R^{\frac{1}{2}}$. Thus, the pressure drag coefficient at low Reynolds number is

$$C_{DP}(\infty, R^{\frac{1}{2}}) = (1{\cdot}674 + 1{\cdot}096)R^{\frac{1}{2}} = 2{\cdot}770R^{\frac{1}{2}}. \tag{6.3}$$

We note that about 60 % of the pressure drag is concentrated at the leading edge.

At high Reynolds numbers, figure 6 indicates a limiting value of about 2·6 for $\bar{C}_{DP}(\infty, R^{\frac{1}{2}})$. Using (5.10), we find that at high Reynolds numbers

$$C_{DP}(\infty, R^{\frac{1}{2}}) = 1{\cdot}57R + 2{\cdot}6R^{\frac{1}{2}}. \tag{6.4}$$

The second term is the second-order boundary-layer contribution which could be checked with a second-order boundary-layer calculation, if one were available.

For purposes of comparison, it would be useful for complete second-order boundary-layer calculations to be made.

We notice from figure 6 that the coefficient of the second term in (6.4) only varies from about 2·9 to 2·6 for the whole Reynolds number range. Thus, we can write an expression

$$C_{DP}(\infty, R^{\frac{1}{2}}) = 1{\cdot}6R + 2{\cdot}8R^{\frac{1}{2}}, \tag{6.5}$$

which is approximately valid for all Reynolds numbers. In the Reynolds number range near zero Reynolds number where the second term in (6.5) is important, 2·8 is a good value for the coefficient. Above a Reynolds number of ten the second term in (6.5) becomes less important.

At zero Reynolds number (the flat plate case) the value of $\bar{C}_{Df}(\infty, R^{\frac{1}{2}})$ obtained from (5.12) should be 2·33, which is an exact value obtained from momentum considerations by Imai (1957).† The value obtained here is 2·41 from taking 40 steps in the ξ direction. The value obtained from taking 20 steps in the ξ direction is 2·58 and thus it appears that more steps in the ξ direction would bring the results closer to Imai's value.

Since there is some of the first-order contribution at high Reynolds number in the $\bar{C}_{Df}(\infty, R^{\frac{1}{2}})$ expression (5.11), this function will go to infinity like $R^{\frac{1}{2}}$ for high Reynolds numbers. Thus in figure 5 we plot the results by dividing by $1 + R^{\frac{1}{2}}$, which removes most of the variation with Reynolds number. The result is not as useful as the pressure drag result since it does not give the second-order boundary-layer friction drag result directly as Reynolds number goes to infinity.

Van Dyke (1972) has used his (Van Dyke 1964) second-order boundary-layer results along with the flat plate results of van de Vooren & Dijkstra (1970) and Yoshizawa (1970) to form a rational fraction for skin friction which approaches the proper limits for skin friction for high and low Reynolds numbers. The expression which results is

$$g(0, R^{\frac{1}{2}}) = \frac{1{\cdot}233 + 2{\cdot}30R^{-\frac{1}{2}}}{1 + 4{\cdot}32R^{-\frac{1}{2}}}. \tag{6.6}$$

Figure 1 shows a comparison of (6.6) with the results obtained here. The results compare well, especially at high Reynolds numbers. The results of Dennis & Walsh (1971) and the local similarity results (see Davis 1967) are presented for comparison. The results of Botta *et al.* (1971) are not shown since they plot precisely on the curve of the present results. The present results should compare better with Van Dyke (1972) at high Reynolds numbers than at low Reynolds numbers since his high Reynolds number expansion is valid to second order, whereas his low Reynolds number expansion is only valid to first order. Table 2 gives a comparison of the results obtained here with those of Dennis & Walsh (1971) and Botta *et al.* (1971). We note that there is almost perfect agreement between the present results and those of Botta *et al.* (1971) and Dennis & Walsh (1971).

We can form a similar expression for $\bar{P}(0, R^{\frac{1}{2}})$. There is no second-order

† D. Dijkstra has pointed out to the author in a private communication that Imai's analysis can be extended to the parabola case to give

$$\bar{C}_{Df}(\infty, R^{\frac{1}{2}}) + C_{DP}(\infty, Re)^{\frac{1}{2}} = \tfrac{1}{2}\pi(1{\cdot}21678 + R^{\frac{1}{2}})^2.$$

The present results are in good agreement with this.

boundary-layer contribution to pressure at the stagnation point so (5.1) gives for high Reynolds numbers

$$\bar{P}(0, R^{\frac{1}{2}}) = 0{\cdot}50 - 1{\cdot}233R^{-\frac{1}{2}}. \tag{6.7}$$

The low Reynolds number leading edge result is

$$\bar{P}(0, R^{\frac{1}{2}}) = 0{\cdot}121. \tag{6.8}$$

	$g(0, R^{\frac{1}{2}})$		
R	Present results	Botta *et al.* (1971)	Dennis & Walsh (1971)
0	0·533	0·534	—
0·1	0·563	0·564	—
1	0·629	0·630	0·627
10	0·793	0·794	0·793
100	1·009	1·010	1·007
1000	1·150	1·148	1·149
10000	1·209	1·206	—

TABLE 2. Comparison with other results

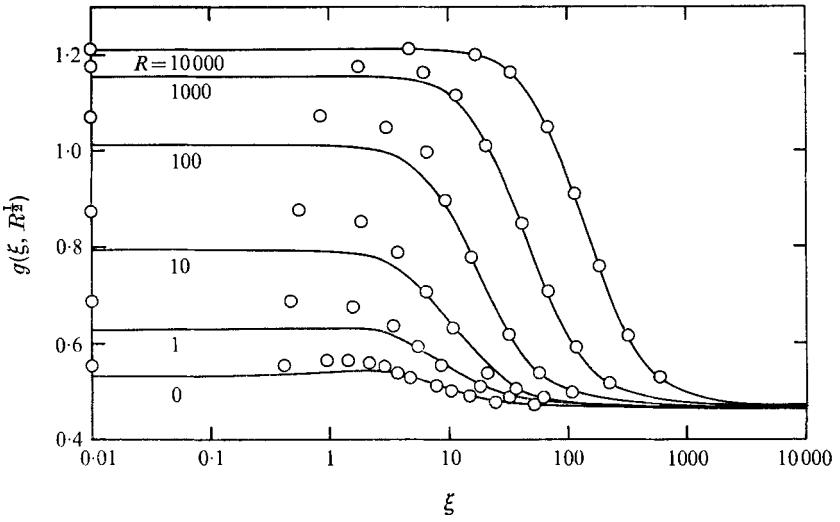

FIGURE 3. Skin friction distribution on a parabolic cylinder. ○, parabolic approximation.

Combining (6.7) and (6.8) to form a rational fraction as was done by Van Dyke (1971) for skin friction gives

$$\bar{P}(0, R^{\frac{1}{2}}) = \frac{0{\cdot}5 + 0{\cdot}393R^{-\frac{1}{2}}}{1{\cdot}0 + 3{\cdot}25R^{-\frac{1}{2}}}. \tag{6.9}$$

Figure 2 shows the same kind of agreement between the rational fraction (6.9) and numerical results for pressure as was found in figure 1 for skin friction.

Figures 3 and 4 show distributions of skin friction and pressure over parabolas at various Reynolds numbers. The results labelled 'parabolic approximation' are obtained by making the governing equations parabolic in ξ. This is done by

neglecting the time derivative in (2.9) and also the last two terms in (2.9) and (2.10), i.e. $g_{\xi\xi}+2g_{\xi}/\xi$ and $f_{\xi\xi}+2f_{\xi}/\xi$. These results are identical to the local similarity results of Davis (1967) at the leading edge and are only slightly different downstream. The difference is due to the inclusion of the parabolic term in ξ in (2.9) in the present results. This term becomes more important at high Reynolds numbers since then the approximation equations including this term reduce to the boundary-layer equations. Comparisons with the more exact numerical solutions to the full Navier–Stokes equations show good agreement downstream for all Reynolds numbers. The agreement is poorest at intermediate Reynolds numbers as indicated in figure 3. The 'parabolic approximation' is the solution that is used as the initial solution for the full time-dependent Navier–Stokes solution. The fact that it is quite close to the exact solution for all Reynolds numbers is one of the reasons the time-dependent method converges rapidly.

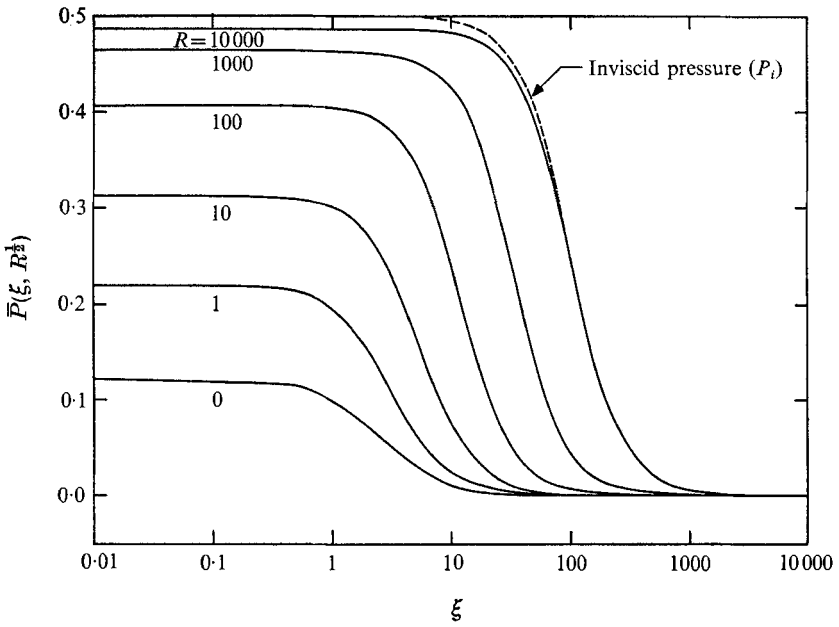

FIGURE 4. Pressure distribution on a parabolic cylinder.

Figure 4 shows a comparison with the inviscid pressure distribution given by (5.8) for the case of a Reynolds number of 10000. Most of the difference in the two results at the leading edge is due to the first term on the right-hand side of (5.4). Since there is no second-order boundary-layer contribution at the leading edge, this correction is all that is needed at the leading edge to second order. However, since there is a second-order correction in pressure downstream on the parabola, an additional correction is needed there, which has not been found until the present. It is interesting to note that ignoring the second-order boundary-layer correction but including the first term in (5.4) gives good agreement with the numerical results for all positions on the parabola. Evidently, the second-order boundary-layer correction is quite small. Comparison of skin friction with first-order boundary-layer theory shows similar agreement.

A final set of calculations was made in which the last two terms in (2.9) were neglected (i.e. $g_{\xi\xi}+2g_{\xi}/\xi$) while the last two terms in (2.10) were retained (i.e. $f_{\xi\xi}+2f_{\xi}/\xi$). One would expect that this might be a good approximation since g dies out exponentially far from the body whereas f dies out algebraically. This was pointed out in § 2 where it was mentioned that local similarity does not properly handle the algebraic decay of f. We might interpret the inclusion of the $f_{\xi\xi}+2f_{\xi}/\xi$ terms as a displacement correction. Numerical results obtained using this approximation are almost identical for all Reynolds numbers with the solution to

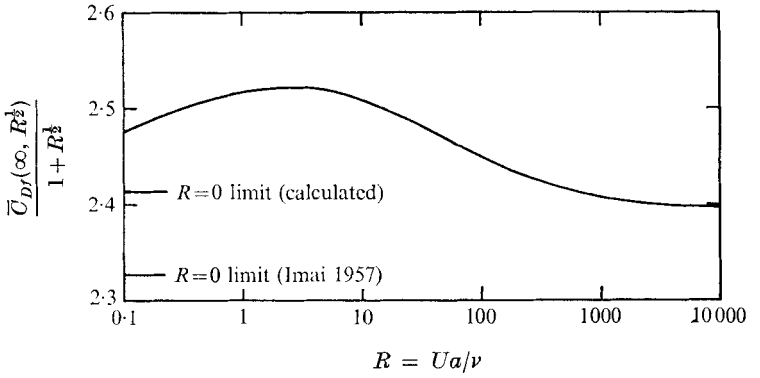

FIGURE 5. Friction drag coefficient on a parabolic cylinder.

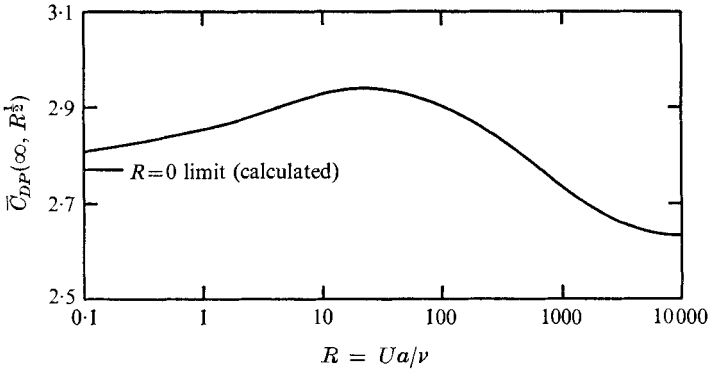

FIGURE 6. Pressure drag coefficient on a parabolic cylinder.

the full equations. In fact, to the scale of all of the plots given in this paper, no difference can be detected. Thus, one is led to the conclusion that most of the difference between the exact results and the 'parabolic approximation' (which gives results close to local similarity) is due to displacement effects, even at low Reynolds numbers. These results indicate that it is possible to use a set of equations simpler than the full Navier–Stokes equations for calculating flow fields which will give accurate solutions at all Reynolds numbers. Use of a proper coordinate system in doing this is undoubtedly important. In high speed viscous flows, approximations of the same type have been made, for example, by Cheng (1963), Davis (1970), and Cheng *et al.* (1970). Approximations of this type which make the momentum or vorticity equations parabolic can lead to considerable

simplifications in numerical schemes and save large amounts of computing time over solutions of the full Navier–Stokes equations. These solutions may in fact give results which are accurate to lower values of Reynolds number than an order-of-magnitude analysis would suggest.

In conclusion, it must be said that, in cases where direct comparisons can be made with the classical second-order boundary-layer theory of Van Dyke (1964), the results are disappointing. One would hope that second-order boundary-layer theory would give good results to Reynolds numbers of at least 100 for the present case. Figure 1, for example, shows that the results diverge at much higher Reynolds numbers. There is always the possibility of a mistake in the results of Van Dyke or the results presented here; however, the good agreement between the present numerical results and the rational fractional approximation (which contains the second-order boundary-layer results) indicates that both results are probably correct. The need for further work on finding the complete second-order boundary-layer solution for flow over the entire parabola is thus obvious. One should be able to determine from this solution which terms are responsible for the poor agreement with the Navier–Stokes solutions.

This work was supported by the Office of Naval Research under Contract N0014-70-C-0024 Task 061-180. The author is indebted to Milton Van Dyke, M. J. Werle, S. C. R. Dennis, D. Dijkstra, F. G. Blottner, and P. J. Roache for valuable comments and suggestions.

REFERENCES

BLOTTNER, F. G. & FLÜGGE-LOTZ, I. 1963 *J. de Mécanique*, **2**, 397–423.
BOTTA, X., DIJKSTRA, D. & VELDMAN, J. 1971 To appear in *J. Engng. Math.*
CHENG, H. K. 1963 *Cornell Aero. Lab. Report*, no. AF-1284-A-10.
CHENG, H. K., CHEN, S. H., MOBLEY, P. & HUBER, C. P. 1970 *Rand Report*, RM-6193-PR.
DAVIS, R. T. 1967 *J. Fluid Mech.* **27**, 691–704.
DAVIS, R. T. 1970 *A.I.A.A. J.* **8**, 843–851.
DEAN, W. R. 1954 *Mathematika*, **1**, 443–456.
DENNIS, S. C. R. & CHANG, G. Z. 1969 *Phys. Fluids Supp.* II, II-88-93.
DENNIS, S. C. R. & WALSH, J. D. 1971 *J. Fluid. Mech.* **50**, 801–814.
DIJKSTRA, D. 1969 *Mathematisch Instituut Rijksuniversiteit Groningen Report*, TW-72.
DOUGLAS, J. 1955 *J. Soc. Indust. Appl. Math.* **3**, 42–65.
IMAI, I. 1957 *Aeron. Sci.* **24**, 155–156.
THOMAS, L. H. 1949 *Watson Science Computing Lab. Report*, Columbia University.
VAN DYKE, M. 1964 *J. Fluid Mech.* **19**, 145–159.
VAN DYKE, M. 1972 Submitted to *J. Fluid Mech.*
VAN DE VOOREN, A. I. & DIJKSTRA, D. 1970 *J. Engr. Math.* **4**, 9–27.
YOSHIZAWA, A. 1970 *J. Phys. Soc. Japan*, **28**, 776–779.